

2004

In vivo dosimetry and seed localization in prostate brachytherapy with permanent implants

Anatoly B. Rosenfeld

University of Wollongong, anatoly_rozenfeld@uow.edu.au

D. L. Cutajar

University of Wollongong

M. L. Lerch

University of Wollongong, mlerch@uow.edu.au

G. J. Takacs

University of Wollongong, git@uow.edu.au

J. Brady

*University of Wollongong**See next page for additional authors*

Publication Details

This paper originally appeared as: Rosenfeld, AB, Cutajar, DL, Lerch, ML et al, In vivo dosimetry and seed localization in prostate brachytherapy with permanent implants, IEEE Transactions on Nuclear Science, December 2004, 51(6)1, 3013-3018. Copyright IEEE 2004.

Authors

Anatoly B. Rosenfeld, D. L. Cutajar, M. L. Lerch, G. J. Takacs, J. Brady, T. Braddock, V. Perevertailo, J. Bucci, J. Kersley, M. Zaider, and M. Zelefsky

In Vivo Dosimetry and Seed Localization in Prostate Brachytherapy with Permanent Implants

A.B. Rosenfeld, *Senior Member, IEEE*, D.L. Cutajar, M.L.F. Lerch, *Member IEEE*, G.J. Takacs, J. Brady, T. Braddock, V. Pervertailo, *Member, IEEE*, J. Bucci, J. Kersley, M. Zaider and M. Zelefsky

Abstract—This paper reports on the development of an interactive, intraoperative dose planning system for seed implant brachytherapy in cancer treatment. This system involves in-vivo dosimetry and the ability to determine implanted seed positions. The first stage of this project is the development of a urethral alarm probe to measure the dose along the urethra during a prostate brachytherapy treatment procedure. Ultimately the system will be used to advise the physicians upon reaching a preset dose rate or dose after total seed decay in urethra during the seed placement. The second stage is the development of a method and instrumentation for in-vivo measurements of the location of implanted seeds in the same frame as for dose planning, and using these in intraoperative treatment planning. We have developed a silicon mini-detector and preamplifier/amplifier system to satisfy the spectroscopic requirements of the urethral probe. This technique will avoid complications related to overdosing the urethra and the rectum.

I. INTRODUCTION

REAL-TIME transrectal ultrasound guided transperineal placement of permanent interstitial ^{125}I and ^{103}Pd sources is one of the treatment modalities available for early stage prostate cancer. There has been a rapid expansion of the use of this procedure, which is set to become the most common treatment modality for early stage prostate cancer. Equivalent biochemical control rates for low risk prostate cancer with permanent seed implantation in comparison to radical prostatectomy or external beam radiotherapy have been confirmed [1,2]. These biochemical outcomes have been favourable, but there has been little emphasis on the evaluation and comparison of side effects and complications. Interstitial

brachytherapy exhibits a different side effect profile than radical prostatectomy or external beam radiotherapy. Specifically, acute urinary side effects predominate in interstitial prostate brachytherapy [3,4,5]. Urinary symptoms, resulting in an increase of the International Prostate Symptom Score (IPSS), are well-recognized side effects of interstitial prostate brachytherapy, however more detailed evaluation of these symptoms has been lacking. Wallner et al. [6] observed an increase in grade-3 late urethral toxicity when the urethral dose exceeded 400Gy. Recent recommendations by the American Brachytherapy Society (ABS) for reporting morbidity after prostate brachytherapy, request urethral doses be recorded for correlation with urethral toxicity [7]. The ABS recommends that doses be obtained at the centre of the urethra, in half-centimeter intervals, from the base to the apex of the prostate, reporting the maximum and mean obtained doses [7].

Medical complications associated with interstitial prostate brachytherapy can result from errors in seed placement during insertion. There are several factors that may lead to the misplacement of seeds. The guiding needles may diverge during insertion as different layers of tissue are penetrated [8], resulting in the incorrect deposition of seeds, the seeds may drift along the path of the needles, blood flow may alter the seed positions, oedema may alter the size and shape of the prostate, and gland motion may occur [9]. There is a need for seed locations to be monitored in real-time during insertion (intraoperatively). If a seed is misplaced, the required locations of other seeds may be recalculated in compensation. Intraoperative localization of inserted seeds will also provide a method of online dosimetry. Many difficulties have been encountered in the development of an inter-active planning system in the operating theatre in prostate brachytherapy [10]. Current commercial systems use ultrasound visualization of individual seeds or needles to predict the dose within the prostate during treatment [11]. These systems are expensive, have problems with artifacts as on 2D ultrasound seed imaging and are unable to precisely determine individual seed placement during a treatment procedure. The Memorial Sloan-

Manuscript received October 29, 2003.

Authors A.B. Rosenfeld, M.L.F. Lerch, G.J. Takacs, D.L. Cutajar, J. Brady and T. Braddock, Centre for Medical Radiation Physics, University of Wollongong, Wollongong, Australia

V. Pervertailo, SPA-BIT, Kiev, Ukraine

J. Bucci, J. Kersley, Institute for Prostate Cancer, St George Cancer Care Centre, Kogarah, Australia

M. Zaider, M. Zelefsky, Memorial Sloan-Kettering Cancer Center, New York, New York

Kettering Cancer Center (MSKCC) has developed an intraoperative conformal optimization and planning system (I-3D) for ultrasound-based transperineal prostate implants [12]. Optimal operation of this system requires accurate and reproducible real-time position co-ordinates of each successively implanted seed. The MSKCC has also recently developed an intraoperative dosimetry system for prostate brachytherapy based on the combination of two imaging techniques [13]. Ultrasound images are obtained of the prostate and lead markers. Fluoroscopic images of the implanted seeds and lead markers are also obtained. The seed locations obtained from the fluoroscopic images are superimposed onto the prostate images using computer reconstruction. The entire process takes approximately 10 minutes [13].

Here we propose the development of an alternative intraoperative dosimetry system based on miniature solid-state detectors used in spectroscopy mode. Brachytherapy seeds contain radioactive sources, usually ^{125}I or ^{103}Pd . These radioactive sources emit low energy photons with a distinct energy spectrum, at very low dose rates that are hard to measure with conventional detectors in confined spaces. The ability of solid-state detectors to resolve these energies is improving as new detector technologies are being developed. At these low energies, approximately 27 keV for ^{125}I , most energy loss occurs through the photoelectric effect. The Compton scattering cross-section is significant, but energy loss due to the Compton effect is minimal. The attenuation coefficient for low energy photons in tissue decreases with an increase in energy. Spectral peaks of different energies will be attenuated by different amounts as the emitted photons penetrate the tissue. Using this principle, the ratio of peak heights or area under the peaks in an obtained spectrum will yield the distance from a measured seed to the detector. If the distance to one detector is known, the triangulation of distances from a non-coplanar array of detectors will yield the seed position. Such a system will be intraoperative, and will allow online dosimetry of the treatment.

II. MATERIALS AND METHODS

Monte Carlo simulations and experimental measurements were performed on an OncoSeed number 6711 from Amersham Health [14]. This seed consists of radioactive ^{125}I , absorbed onto a silver rod, encapsulated in a hollow titanium cylinder with welded ends. The geometry of the seed was obtained from Williamson [15]. The silver rod is 3mm in length and 0.5mm in diameter. A 1-micrometer thick coating of silver halide is present on the rod. The radioactive iodine was assumed to be at the midpoint of the silver halide coating. The titanium shell was 4.5mm in length, 0.8mm in diameter, was 0.06mm thick along the sides and 0.5mm thick at the end welds. ^{125}I decays via electron capture, emitting photons of several distinct energies through gamma and X-ray emission. Internal conversion and Auger electrons are also emitted, but

were neglected, as they would not penetrate the titanium shell. A 3.6keV photon was also neglected.

TABLE I
6711 SEED PHOTON EMISSION [16]

Energy (keV)	Mean number/disintegration
35.492	0.0666
31.877	0.0438
30.980	0.201
27.472	0.756
27.202	0.405

Due to the presence of silver in the seed, silver fluorescent X-rays of energies 22.1keV and 25.2keV are also present [17].

Monte Carlo simulations were performed using EGSnrcV2 [18]. The FLURZnrc user code was used to simulate the 6711 seed in a liquid water phantom. The energy spectrum was obtained at various locations for distances up to 5cm from the seed centre at various angles around the seed. The area under each photon peak was measured for each obtained spectrum. The ratios of peak areas were calculated for the 27keV peak, the 31keV peak and the 35keV peak. These obtained peak ratios were plotted vs. distance from the seed and angle about the seed axis. An algorithm relating peak ratio to seed location was then constructed.

Given that we have a method for determining the distance from a seed to a detector, if we have four or more non-coplanar detectors, we can then determine the location of the seed. For example, if we have 'n' detectors, each at a known location \mathbf{r}_i , and the distance between a seed and each detector determined from analysis of the spectrum is s_i , then we may determine the seed location from minimization of the following function

$$\sum_{i=1}^n \{(\mathbf{r} - \mathbf{r}_i) \bullet (\mathbf{r} - \mathbf{r}_i) - s_i^2\} \quad (8)$$

The location \mathbf{r} , which minimizes this, is then the estimate of the seed location.

III. RESULTS

From Fig. 2 it can be seen that the photon peaks in the energy spectrum of the 6711 seed are very sharp, with very little scattering, even after the photons have traversed 5cm of liquid water. This allows the use of spectroscopy for analyzing the radiation throughout the prostate during interstitial brachytherapy. The areas under the 27keV, 31keV and 35keV peaks were measured for each obtained spectra and plots of ratio vs. distance along the transverse axis of the seed were obtained.

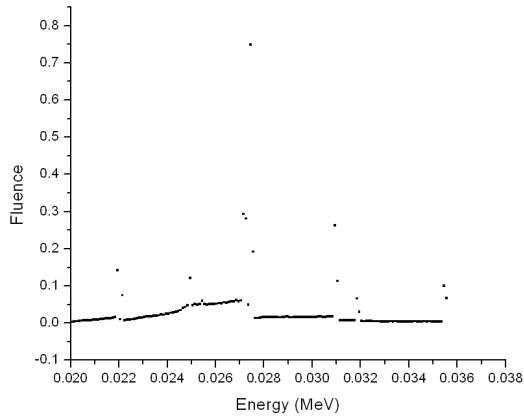


Fig. 2. FLURZnrc energy spectrum of 6711 seed, measured 5cm from seed along the transverse axis.

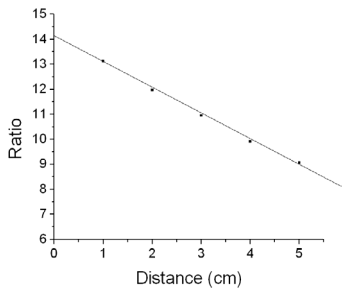


Fig. 3. Ratio of the area under the 27keV peak to the area under the 35keV peak vs. distance along the transverse axis for the 6711 seed, obtained from the FLURZnrc spectra.

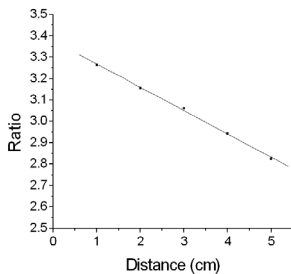


Fig. 4. Ratio of the area under the 31keV peak to the area under the 35keV peak vs. distance along the transverse axis for the 6711 seed, obtained from the FLURZnrc spectra

Since scattering is minimal and the majority of energy loss occurs through the photoelectric effect the area under each peak as a function of distance may be given by

$$A = A_0 e^{-\mu r} / r^2 \quad (1)$$

where A is the area under a single peak, A_0 is the area at zero distance, μ is an effective attenuation coefficient of the medium for photons of the peak energy and r is the distance

from the seed to the point of measurement. The ratio of the area under two peaks, a and b, may be given by

$$R^{a/b} = R_0^{a/b} e^{-\Delta\mu r} \quad (2)$$

where $R^{a/b}$ is the ratio of the area under peak a to the area under peak b, $R_0^{a/b}$ is the peak ratio at zero distance and $\Delta\mu$ is the difference in attenuation coefficients ($\mu_a - \mu_b$). Using (2) and the data obtained from the FLURZnrc simulations of the 6711 seed in water, the following equations were devised.

$$R^{27/35} = 14.41 e^{-0.093r} \pm 3\% \quad (3)$$

$$R^{31/35} = 3.39 e^{-0.036r} \pm 4\% \quad (4)$$

The distance to a 6711 seed within liquid water may be calculated by measuring the ratio of the area underneath two peaks in the spectrum and using (3) or (4). This assumes the point of measurement is along the transverse axis of the seed.

The previous calculations were repeated for spectra obtained at different angles around a 6711 seed in a water phantom. A plot of $R^{27/35}$ vs. distance was obtained in Fig. 5.

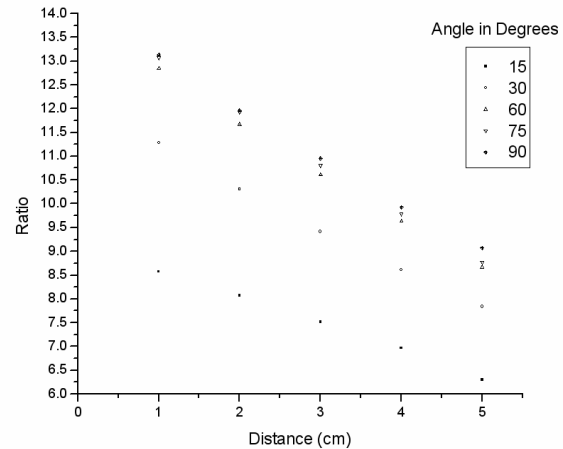


Fig. 5. The ratio of the area under the 27keV peak to the area under the 35keV peak vs. distance for a 6711 seed in a water phantom, calculated at various angles around the seed. 90° represents measurements along the transverse axis of the seed

It can be seen that the peak ratios vary with changes in source angle. This is due to the variation in thickness of the titanium shell around the seed. Photons at lower angles traverse a greater thickness of titanium, increasing the attenuation, lowering the peak ratios. Simply finding the ratio of any two peaks in a measured spectrum is not enough to determine the distance to the seed. The peak ratios are a function of both distance and angle. Assuming the distance from the source is the order of centimeters the peak ratios may be represented as separable functions of both distance and angle,

$$R = R_0 f(r) g(\theta) \quad (5)$$

where $f(r)$ is the distance dependent function of the peak ratio and $g(\theta)$ is the angular dependent function of the peak ratio.

$f(r)$ was previously found to be $e^{-\Delta\mu r}$. To determine the angular dependent function of the peak ratios, $g(\theta)$, the peak ratios vs. angle were plotted for a fixed distance of 1cm, and normalized.

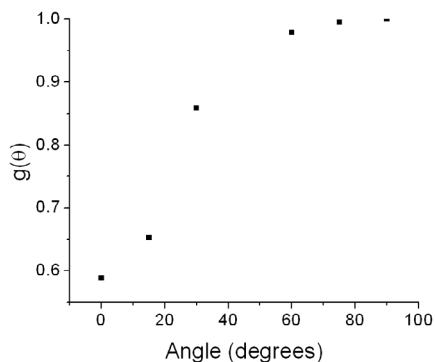


Fig. 6. Normalized plot of $R^{27/35}$ vs. angle to determine the function $g(\theta)^{27/35}$. Ratios were calculated 1cm from the seed centre.

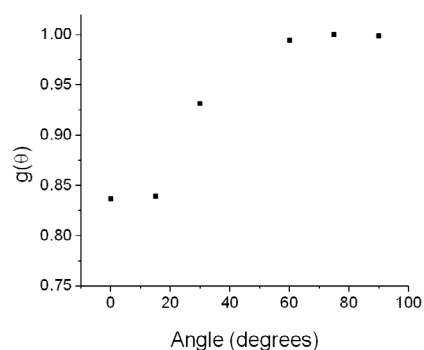


Fig. 7. Normalized plot of $R^{31/35}$ vs. angle to determine the function $g(\theta)^{31/35}$. Ratios were calculated 1cm from the seed centre.

After taking into account the angular variance in peak ratios, (3) and (4) become

$$R^{27/35} = 14.41e^{-0.093r} g(\theta) \pm 5\% \quad (6)$$

$$R^{31/35} = 3.39e^{-0.036r} g(\theta) \pm 6\% \quad (7)$$

By calculating the area under the 27keV, 31keV and 35keV peaks for an obtained spectrum, performing ratios of the obtained areas and solving (6) and (7) simultaneously, the distance to the seed as well as the angle of the seed to the point of measurement may be determined.

In order to determine the practicality of this approach for determining seed positions we have conducted simulations where seeds are placed at random in a specified cubical volume. Four detectors are placed in a tetrahedral configuration. The distances between each detector and a given seed are determined. These distances are then varied randomly to simulate the effects of noise and uncertainties due to seed anisotropy, etc. These uncertain distances are then used, along with the known detector positions, in the equation (8) above. The position r , which minimizes this, is determined by the

downhill simplex method [19], and compared to the seed location. The accuracy of this method for locating seeds is a function of treatment volume, tetrahedron size, and the assumed magnitude of uncertainties in seed-detector distances. Table II gives results for trials of one million seed positions in cubes of various edge lengths. These have been chosen to span the range of treatment volumes, even though the shape differs from a typical prostate.

The results of Table II show that the proportion of times that a large seed location error occurs is sensitive to the precision with which the seed-detector distances can be determined. An increase in this by a factor of 2.5 results in an increase by the same factor in the average error, but the proportion of times an error of greater than 2.5mm occurs increases by a much greater factor.

TABLE II
ERRORS IN SEED LOCATION

Cube edge length (mm)	Tetrahedron edge length (mm)	Average error (mm)	Percentage greater than 2.5mm	Error (%) in seed-detector distance
4.5	3.0	1.8	18	5
4.0	3.0	1.6	12	5
3.5	2.5	1.4	7	5
3.0	2.5	1.2	3	5
4.5	2.5	0.72	0.12	2
4.0	2.5	0.63	0.011	2
3.5	2.5	0.56	0.0003	2
3.0	2.5	0.49	0.0012	2

Stage 1 in the development of an in vivo dosimetry and seed localization system is the construction of the urethra alarm probe. This uses spectroscopy to estimate the dose to the urethra during interstitial brachytherapy treatment. The probe consists of a silicon mini-detector of dimensions 0.8mm x 0.8mm x 3mm. This is connected to a preamplifier/amplifier system by a thin 40cm cable, allowing the placement of the detector within the prostate via a urinary catheter. The probe was used to measure the spectrum of a 6711 seed in air at 25°C, while connected to the amplifier system via a 40cm cable that would be used in practice.

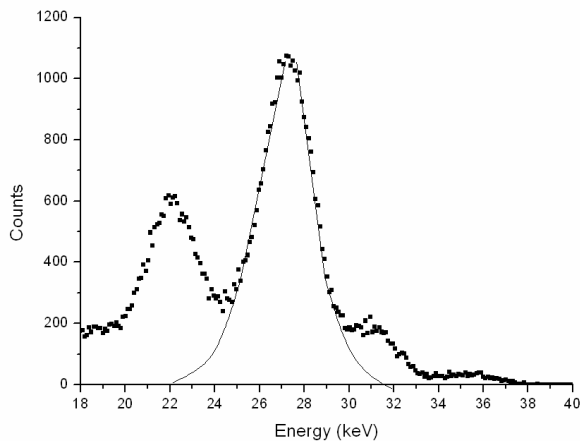


Fig. 8. 6711 seed spectrum, measured with the Urethra Alarm Probe connected to the preamplifier via a 40cm cable. The 27keV peak is well resolved. The 31keV and 35keV peaks are well resolved but do not contain many counts. Also present is the 22keV silver X-ray peak. The 27keV peak is outlined and has a FWHM of 2.3keV

The 6711 seed spectrum in Fig. 8 shows that the current detector system does not accurately resolve the peaks necessary for use in seed localization. It does, however, show that the current system may be used for dosimetry purposes. The 27keV peak is well resolved. Since scattering is minimal and most energy loss is due to the photoelectric effect, the area under the 27keV peak may be used to estimate the dose received by the detector. The probe may be placed inside the prostate during seed insertion to allow the physicians to ensure the dose received by the urethra is within tolerable limits. The photon spectrum of the 6711 seed was also measured with the photons incident on the rear of the detector. There was no apparent change in the measured spectrum, indicating that the detector was fully depleted and has an isotropic response to photon irradiation.

IV. CONCLUSION

The development of an intraoperative treatment planning system for low dose rate brachytherapy of the prostate, based on semiconductor detectors operating in spectroscopy mode, seems to be feasible. Such a system will allow updating of the treatment plan to correct for seed misplacement, and online dosimetry. A method exists for locating seeds, based on distances between four detectors and a seed, with each of these distances being determined by observation of the ratio of counts under different energy peaks. The determination of the distance from a seed to a detector is possible theoretically but has yet to be proven experimentally.

V. REFERENCES

- [1] J.C. Blasko, P.D. Grimm, J.E. Sylvester et al, "Palladium-103 brachytherapy for prostate carcinoma", *Int J Radiat Oncol Biol Phys*, 2000, vol 46, pp 839-850.
- [2] H. Ragde, A. A. Elgamal, P.B. Snow et al, "Ten-year disease free survival after transperineal sonography-guided iodine-125 brachytherapy with or without 45-gray external beam irradiation in the treatment of patients with clinically localized, low to high Gleason grade prostate carcinoma", *Cancer*, 1998, vol 83, pp 989-1001.
- [3] D.Y. Gelblum, L. Potters, R. Ashley et al, "Urinary morbidity following ultrasound-guided transperineal prostate seed implantation", *Int J Radiat Oncol, Biol, Phys*, 1999, vol 45, pp 59-67
- [4] N. Lee, C. Wu, R. Brody et al, "Factors predicting for postimplantation urinary retention after permanent prostate brachytherapy", *Int J Radiat Oncol Biol Phys*, 2000, vol 48, pp 1457-1460.
- [5] G.S. Merrick, W.M. Butler, J.H. Lief, and A.T. Dorsey, "Temporal resolution of urinary morbidity following prostate brachytherapy", *Int J Radiat Oncol, Biol Phys*, 2000, vol 47, pp 121-128.
- [6] K. Wallner, J. Roy and L. Harrison, "Dosimetry guidelines to minimize urethral and rectal morbidity following transperineal I-125 prostate brachytherapy", *Int J Radiat Oncol Biol Phys*, 1995, vol 32, 465-471.
- [7] S. Nag, R.J. Ellis, G.S. Merrick, R. Bahnson, K. Walner, R. Stock, "American Brachytherapy Society (ABS) Recommendations for reporting morbidity after prostate brachytherapy", *Int J Radiat Oncol Biol Phys*, 2002, Vol.54, N2, pp.462-470.
- [8] S. Nath, Z. Chen, N. Yue, S. Trumppore and R. Peschel, "Dosimetric effects of needle divergence in prostate seed implant using I-125 and I-131 radioactive seeds", *Medical Physics* 2000, vol 27, no 5, pp 1058-1066.
- [9] R. Taschereau, J. Roy, J. Pouliot, "Monte Carlo simulations of prostate implants to improve dosimetry and compare planning methods", *Medical Physics*, 1999, vol 26, no 9, pp 1952-1959.
- [10] S. Nag, J.P. Ciezki, R. Cormack, S. Doggett, K. DeWynngaert, G.K. Edmundson, R.G. Stock, N.N. Stone, Y. Yu, M.J. Zelefsky, "Intraoperative planning and evaluation of permanent prostate brachytherapy: report of the American Brachytherapy", *Int J Radiat Oncol Biol Phys*, 2001, Dec 1; vol 51(5), pp 1422-1430.
- [11] "SPOT: 3D Ultrasound Brachytherapy Planning, System for Seed Implants", Nucletron brochure, 1999
- [12] M.J. Zelefsky, Y. Yamada, G. Cohen, E.S. Venkatraman, A.Y. Fung, E. Furhang, D. Silvern, M. Zaider, "Postimplantation dosimetric analysis of permanent transperineal prostate implantation: improved dose distributions with an intraoperative computer-optimized conformal planning technique", *Int J Radiat Oncol Biol Phys*, 2000, vol 48, pp 601-608.
- [13] D.A. Todor, M. Zaider, G.N. Cohen, M.F. Worman and M.J. Zelefsky, "Intraoperative dynamic dosimetry for prostate implants", *Phys, Med, Biol*, 2003, vol 48, pp 1153-1171.
- [14] Amersham Health Inc, 101 Carnegie Center, Princeton, NJ 08540-6231, USA, Tel. +1 609 514 6000, Fax. +1 609 514 6660/6572.
- [15] J.F. Williamson, "Monte Carlo evaluation of specific dose constants in water for I-125 seeds", *Medical Physics*, 1988, vol 15, no 5, pp 686-694.
- [16] E. Browne, R.B. Firestone, "Table of radioactive isotopes", edited by V.S. Shirley, John Wiley and Sons, New York, 1986
- [17] Schell et al, "Dose distributions of model 6702 I-125 seeds in water." *Int J Radiat Oncol Biol Phys*, 1997, vol 13, pp 795-799.
- [18] I. Kawrakow and D.W.O. Rogers, The EGSnrc Code System, NRC Report PIRS-701, (NRC, Ottawa, 2000).
- [19] J.A. Nelder and R. Mead, *Computer Journal*, vol. 7, 1965, pp. 308-313